Available online at www.sciencedirect.com
ScienceDirect
Polymer 49 (2008) 1137–1144
polymer
www.elsevier.com/locate/polymer

Synthesis and characterization of 2-D and 3-D covalent networks derived from triazine central cores and bridging aromatic diamines

Panagiotis Dallas [a,*], Athanasios B. Bourlinos [a,*], Dimitrios Petridis [a], Nicholaos Boukos [a], Kyriaki Papadokostaki [b], Dimitrios Niarchos [a], Nicholaos Guskos [c]

[a] *Institute of Materials Science, NCSR ''Demokritos'', Ag. Paraskevi Attikis, Athens 15310, Greece*
[b] *Institute of Physical Chemistry, NCSR ''Demokritos'', Ag. Paraskevi Attikis, Athens 15310, Greece*
[c] *Solid State Section, Department of Physics, University of Athens, Panepistimiopolis 15784, Zografou, Athens, Greece*

Received 23 May 2007; received in revised form 3 January 2008; accepted 15 January 2008
Available online 19 January 2008

Abstract

Nucleophilic substitutions of the reactive chlorine atoms in either cyanuric or phosphonitrilic chloride by the bridging 1,4-phenylenediamine and benzidine units lead to the formation of two- (2-D) or three-dimensional (3-D) covalent networks, according to the spatial arrangement of the chlorine atoms in each particular triazine core. The materials are electrochemically active and stable, and exhibit interesting optical properties. The UV–visible spectral absorptions are significantly red-shifted and can been altered upon chemical oxidation. Furthermore, a three-band absorption spectrum typical of polaronic nature is observed in the case of the layered benzidine/cyanuric chloride network. Either spherical (2-D) or cubic (3-D) morphologies were revealed by SEM analysis, while the XRD patterns indicated partial crystallinity. Due to the inherited ion-exchange properties of the 2-D and 3-D ionic networks, the materials can be regarded as the organic analogues of conventional inorganic layered or zeolitic ion-exchangers.

Keywords: Triazine; Organic nanostructures; Aromatic diamines

1. Introduction

Triazine molecules appear to be of significant importance in the construction of supramolecular organic networks with widespread applications [1–4]. Especially cyanuric chloride has been consistently reported to form supramolecular networks with interesting properties, e.g. optical, after nucleophilic substitution with certain aromatic diamines [2]. More specifically, nucleophilic substitutions of the reactive chlorine atoms in cyanuric chloride by the bridging 4,4′-bipyridine in refluxing toluene have previously led to quaternization of the latter and the subsequent formation of a covalent layered network [2]. The layered network is composed of central 1,3,5-triazine units with 4,4′-bipyridinium rings covalently attached and balanced by the released chloride counterions. Covalently engineered networks of this kind introduce a new class of functional organic materials with fundamental and practical interest in materials science. The method can potentially give access to a wide class of novel triazine-based derivatives by varying the type of the bridging diamine or the triazine core. Furthermore, by manipulating the local chemical environment of a targeted substance via redox and/or ion-exchange reactions it is possible to receive new reconstructed derivatives. In all respects, the affordable structural changes may impart new physical properties in the solid state, like optical or electronic. Besides cyanuric chloride, phosphonitrilic chloride has also been utilized for the construction of various dendritic structures [5]. These lightweight materials are promising candidates for various applications like optical organic materials [6] or nanostructured electronic devices [7].

* Corresponding authors. Tel.: +30 2106503309; fax: +30 2106519430.
E-mail addresses: dallas@ims.demokritos.gr (P. Dallas), bourlinos@ims.demokritos.gr (A.B. Bourlinos).

0032-3861/$ - see front matter © 2008 Elsevier Ltd. All rights reserved.
doi:10.1016/j.polymer.2008.01.030

On the other hand, many scientific studies continue to focus on the synthesis and characterization of various low band gap materials [8] such as thiophene [9], oligoquinoline [7] or xanthene derivatives [10]. Another promising area of application of these conjugated organic materials is their use in the solar cells technology [11], where the efficiency is highly enhanced if a p- and n-type conjugated materials' heterojunction is applied [12]. This field of materials science appears to be of significant interest due to the molecular symmetry, π-interaction ability and charge transfer properties of the conjugated polymers. The band gap of these polyaromatic systems is highly dependent on the electron density of the constituents, the planarity and symmetry of the macromolecules and the intermolecular interactions [13,14]. Furthermore, the tendency of the conjugated molecules to assemble in various morphologies and nanostructures is well known and definitely affects various applications, like the use of conductive polymers as chemical sensors [15].

In the present work we have employed 1,4-phenylenediamine and benzidine as the bridging units with cyanuric and phosphonitrilic chloride acting as the central building blocks. The reactions are performed in refluxing solvents of relatively high boiling point (>100 °C) in order to ensure complete substitution of the chlorine atoms. The symmetry of the reactants finally dictates the growth of two- (2-D) or three-dimensional (3-D) covalent networks with inherited ion-exchange properties, with cyanuric and phosphonitrilic chlorides favouring 2-D and 3-D lattices, respectively. The samples exhibit interesting electrochemical and optical properties, such as reversible redox reactions and low band gap optical excitations. The organic networks structurally mimic traditional inorganic ion-exchangers, like layered double hydroxides (2-D) and zeolites (3-D).

2. Experimental section

2.1. Chemicals

The phosphonitrilic chloride trimer was purchased from Alfa Aesar (98%), cyanuric chloride from Fluka, 1,4-phenylenediamine from Merck (98%) and benzidine from Fluka. Solutions of cyanuric chloride were filtered off prior to reaction.

2.2. Synthesis of cyanuric 2-D networks

The experimental procedure involves the nearly quantitative reaction of cyanuric chloride (180 mg, 0.98 mmol) with either benzidine (538 mg, 3 mmol; sample name: benz/cyan) or 1,4-phenylenediamine (316 mg, 3 mmol; sample name: phd/cyan) in refluxing toluene (40 mL) for 24 h. Each precipitate was isolated by centrifugation, washed with toluene and acetone and finally dried. Yields exceed 85% assuming that the triazine/bridging amine molar ratio is 1:1.5.

2.3. Synthesis of phosphonitrilic 3-D networks

Typically, phosphonitrilic chloride (180 mg, 0.52 mmol) reacts with an excess of 1,4-phenylenediamine (316 mg, 3 mmol) in refluxing xylene (40 mL) for 72 h. The precipitate was isolated by centrifugation, washed several times with toluene and once with acetone and finally dried. The sample is hereafter denoted as phd/ptr. The reaction yield is 80% assuming a triazine/bridging amine molar ratio of 1:3.

2.4. Characterization techniques

X-ray powder diffraction (XRD) patterns were collected on a D-500 Siemens diffractometer (Cu Kα radiation) using background-free holders and a scan rate of 0.03° s^{-1}. Infrared spectra were taken with a FT-IR spectrometer of Bruker, Equinox 55/S model (4000–400 cm^{-1}). The samples were measured in the form of KBr pellets. The optical spectra were recorded on a Shimadzu UV2100 spectrophotometer (200–900 nm) in the solid state or using diluted colloidal dispersions in quartz cuvettes. The DSC thermal analysis traces were obtained with a TA Instruments temperature modulated DSC (Model 2920) with a heating rate of 5 °C min^{-1} under nitrogen. The modulation step was 0.8 °C min^{-1}. The thermogravimetric analysis was performed in a Perkin–Elmer Pyris TGA with a heating rate of 10 °C min^{-1}. For the cyclic voltammetry study a typical three-electrode electrochemical cell was used, connected to a SOLARTRON 1287 potentiostat. All potentials were recorder versus a saturated calomel electrode (SCE). A platinum grid served as the counter electrode while the working electrode was the Pt previously covered with a thin film of the solid. The measurements were performed in a 0.1 M NaCl aqueous solution and at a scanning rate of 50 mV s^{-1}. Scanning Electron Microscopy (SEM) images were recorded by a FEI INSPECT apparatus. For this purpose, the samples were suspended in acetone and sonicated. Drops from a particular suspension were placed on a silicon wafer followed by evaporation of the solvent at ambient conditions. The obtained films were sputtered with gold prior to direct imaging at 20 kV under vacuum.

3. Results and discussion

3.1. Layered 2-D cyanuric derivatives

In both cases, the reaction yield is almost quantitative resulting in either light green (benz/cyan) or light purple (phd/cyan) powders that lack solubility in aqueous or organic solvents, as it is common for conjugate polymeric materials [16]. However, dispersion of benz/cyan in excess of water provides a clear, diluted colloid. The complete nucleophilic replacement of the chlorine atoms of the triazine was evidenced by IR spectroscopy by the absence of the characteristic C–Cl stretching vibration at 850 cm^{-1} (Fig. 1a). Furthermore, the medium band centered at 2600 cm^{-1} is typical of the ammonium cation $-NH_2^+-$, i.e. the bridging diamine units are protonated and balanced by the released chlorine anions, although –NH– groups are also detected from a very weak band at 3200 cm^{-1}. Since the reaction takes place in an excess of diamine, it is reasonable to assume that the edges of the network consist of both non-protonated and protonated pending amine groups. Thus the corresponding sharp $-NH_2$ vibration modes appear at 3420 and 3320 cm^{-1} while the presence of $-NH_3^+$ groups is marked by

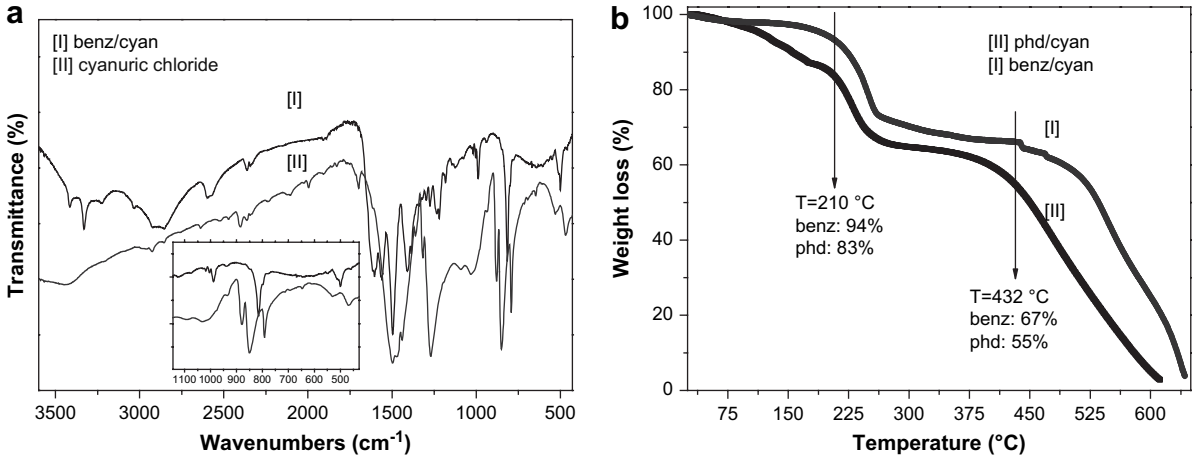

Fig. 1. (a) FT-IR spectrum of the benz/cyan compared to cyanuric chloride. (b) The TGA traces of both cyanuric derivatives.

a broad absorption band at 3000 cm^{-1}. The materials are thermally stable based on their TGA traces under air showing minor weight losses up to 200 °C (Fig. 1b).

The XRD profiles of the two derivatives (Fig. 2) are quite reminiscent of those reported for the 4,4′-bipyridine analogue, thus supporting the growth of layered networks [2,17]. The layered structure is anticipated on account of the planar symmetry of the reactants. The XRD patterns differentiate from the starting crystalline reagents showing instead large amorphous domains that are mainly associated with structural defects and discontinuities within the layers as well as with the disordered stacking of several numbers of individual layers. Nevertheless, the existence of various sharp diffraction peaks in the patterns indicates a partial crystallinity. Characteristically, the pattern of the benzidine derivative is typical for a triazine-based layered structure [2,17] with the additional peak at $2\theta = 25.2°$ (d-spacing = 3.5 Å) implying π–π stacking of phenyl rings among adjacent layers [18]. In contrast, the pattern of phd/cyan lacks this characteristic diffraction peak, thereby suggesting a more amorphous state.

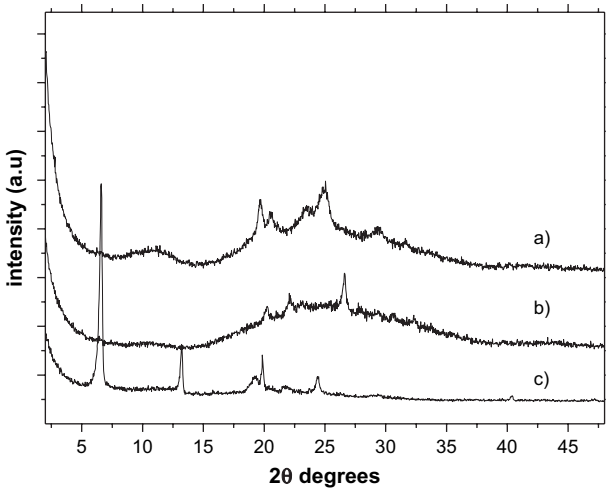

Fig. 2. XRD patterns of (a) benz/cyan, (b) phd/cyan, and (c) benz/cyan after anion exchange with SO_4^{2-}.

The chloride ions deliver exchange properties to the solids allowing the control of the interlayer space with simple or complex anionic species. In the first attempt, sulfate anions (from Na_2SO_4) were used in the exchange process (sample: benz/cyan). The corresponding XRD pattern (Fig. 2) is typical for a layered material exhibiting 1st, 2nd and 3rd order diffractions at the following d-spacings: 13.6 Å ($2\theta = 6.4°$), 6.8 Å ($2\theta = 13.1°$) and 4.5 Å ($2\theta = 19.9°$). The sulfate anions expand the spacing among adjacent layers and simultaneously lead to an ordered stacking. In the second example, the sodium salt of DNA (calf thymus) was used for the anion-exchange intercalation of a biomolecule. Once again, DNA insertion in benz/cyan affords expanded lamellar derivatives with a weak reflection centered at $d = 7$ Å. Due to their layered structure and ion-exchange properties, the materials can be considered as the organic analogues of layered double hydroxides.

Since the bridging units contain amine groups, both materials are expected to be electrochemically active. The cyclic voltammetry diagrams of the corresponding samples (Fig. 3) show that the derivatives are electrochemically stable over many cycles exhibiting two reversible redox peaks. Hence, the two oxidation peaks centered at 0.79/1.22 and 0.23/0.64 V for the benzidine and 1,4-phenylenediamine derivatives, respectively, are accompanied by the corresponding reduction waves centered at 0.45/−0.73 V and 0.66/−0.51 V in the reverse scanning direction. The large shift in the oxidation potential values for benz/cyan may stem from a twisted conformation of the two phenyl rings in benzidine. Each electrochemical step induces certain color changes in the materials that, however, fade gradually with time when the samples are left undisturbed. Besides the instability of the oxidized forms, the samples exhibit similar electrochemical behaviour with polyaniline [19] where also the degree of oxidation greatly influences the displayed optical properties. A schematic of the proposed oxidation steps is shown in Fig. 3. Note that the particular reaction scheme merely focuses on the electrochemically active amine bridges, i.e. the scheme depicts only a part of the 2-D structure. The bonds on the triazine units imply that the 2-D network continues through further bonding with diamine bridges, as it is schematically

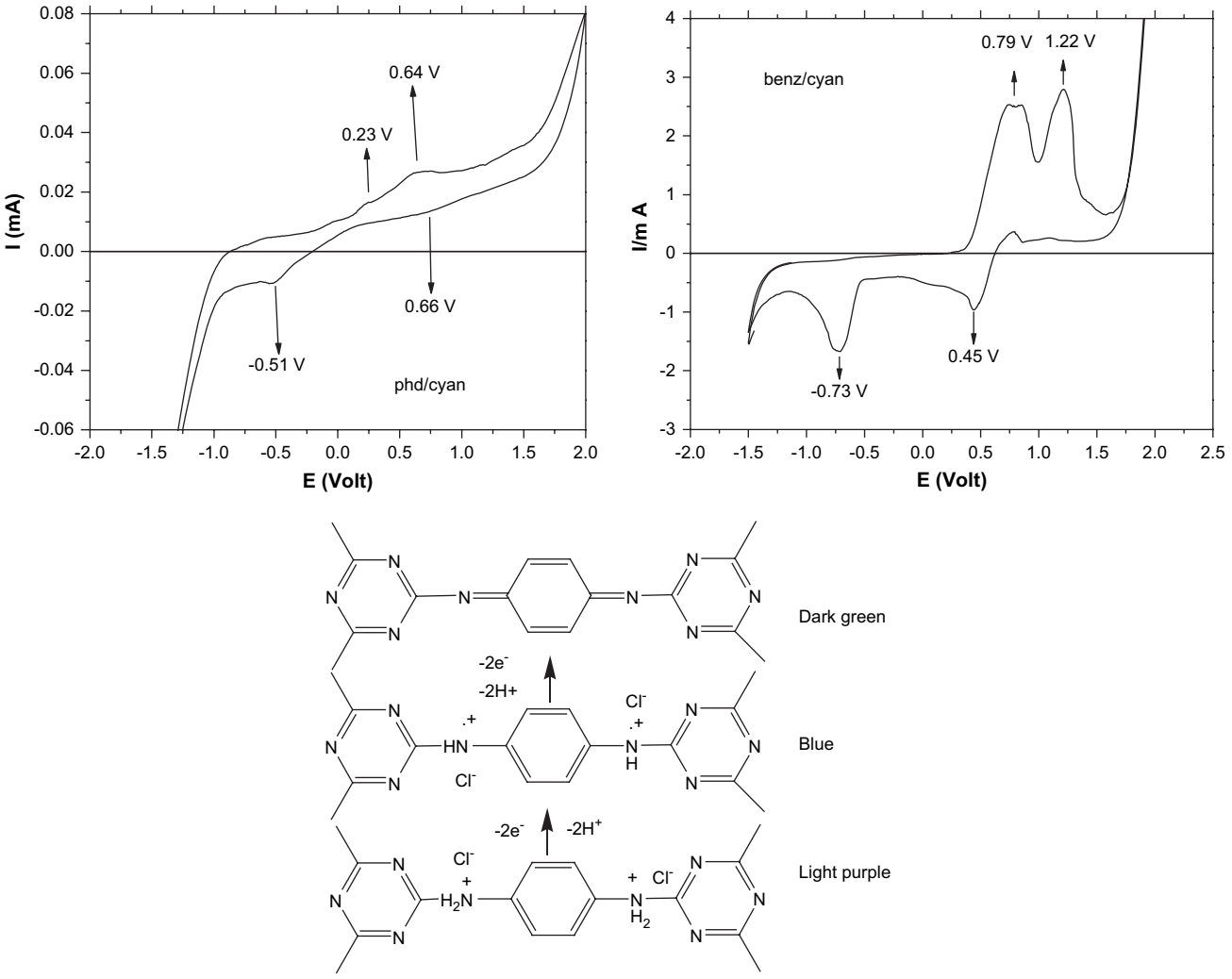

Fig. 3. Cyclic voltammetry diagrams of phd/cyan and benz/cyan samples along with a schematic of the proposed oxidation steps for the former system.

demonstrated for the analogous cyanuric chloride/4,4′-bipyridine couple in Ref. [2]. In the first step, the initial protonated form is oxidized to the radical cation chloride salt. Subsequently, complete removal of the hydrogen atoms leads to the formation of a quinoid structure similar to that previously proposed for the electrochemically active benzidine and 1,4-phenylenediamine rings [20]. A stepwise oxidation of the samples can also be achieved by chemical means, e.g. $(NH_4)_2S_2O_8$. Nevertheless, the reaction seems quite complex heading presumably to different oxidized products. Preliminary studies show that the degree of oxidation is greatly influenced by the amount and type of the oxidant, temperature conditions and reaction time.

SEM study of phd/cyan at different magnifications (Fig. 4) reveals the presence of individual or fused submicrometer-sized grains with a striated surface texture, platy morphology and multi-layered structure at the edges. These features combined are suggestive of a lamella phase formation [21].

The UV–visible spectrum of benz/cyan after high dilution in water (Fig. 5) exhibits distinct absorption peaks centered at the following wavelengths: 833 (energy gap EG = 1.49 eV, π–polaron transition), 607 (EG = 1.94 eV, polaron–π*), 361 nm (EG = 3.43 eV, π–π*) and a small shoulder at 423 nm (EG = 2.93 eV). Note that the optical spectrum may extend at the NIR region, however, this area falls beyond the measuring scale of our UV–visible apparatus. The optical spectrum implies the formation of a low band gap solid with the polaron band arising from delocalized free radicals [22]. These radicals, which are derived from partial air oxidation of the samples near the layers' edges, were evidenced by a sharp EPR line centered at $g \sim 2.0$ [2]. Besides, as it has been previously discussed, the XRD pattern of the benz/cyan sample implies the presence of π–π stacked aromatic units, and thus an increased π electron overlap that facilitates the low band gap excitations [6a]. The 1,4-phenylenediamine derivative lacks solubility in any solvent and thus the spectrum was recorded in the solid state (Fig. 5). In contrast to benz/cyan, the spectrum consists only of a strong absorption centered at 375 nm (EG = 3.30 eV) characteristic of an electron delocalization within the layered network. A small shoulder appears at 530 nm, however, the spectrum does not evidence the formation of a polaron band. Generally, solid-state spectra may obscure subtle information due to intense light scattering and in turn considerable background contribution. Furthermore, the absence of the extra phenyl ring combined with the lack of π–π stacking (based on XRD) may also affect the observed optical transitions.

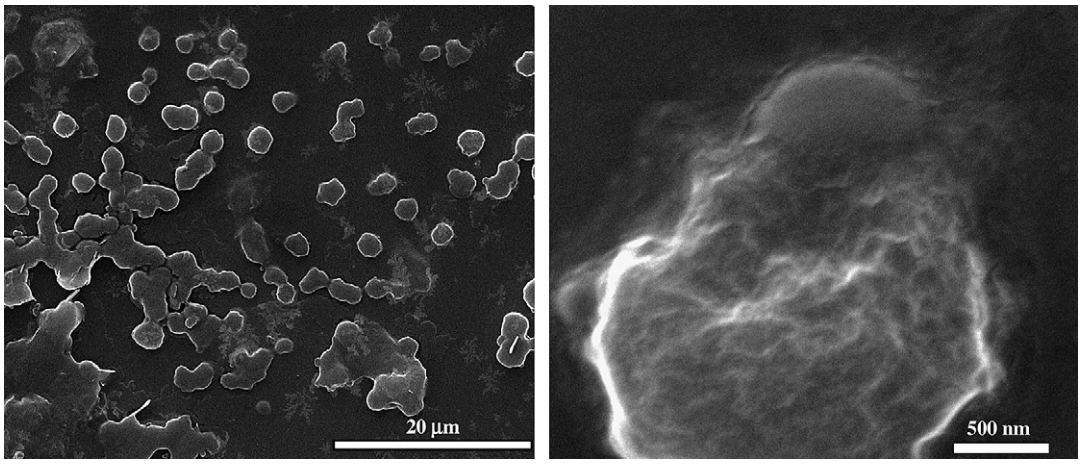

Fig. 4. SEM images of the 1,4-phenylenediamine derivative.

3.2. 3-D phosphonitrilic derivatives

The reaction takes place in refluxing xylene in order to secure complete substitution of the labile chlorine atoms (Scheme 1). A purple powder was isolated, indicating the presence of a minor radical concentration due to partial oxidation of the solid near the surface boundaries. As it is well known, the phosphonitrilic chloride trimer consists of a nearly ''aromatic'' ring with the chlorine atoms located in and out of the ring's plane with a 102° angle between them [23]. The electron delocalization arises between the p orbitals from the nitrogen atoms and the d orbitals from the phosphorus atoms meaning that the electrons are not extensively delocalized alongside the six-membered ring [23]. On account of the spatial arrangement of the chlorine atoms, it is expected that nucleophilic substitution by the symmetric *para*-phenylenediamine will lead to a 3-D covalent network that is balanced by the released compensating chloride ions.

The material was characterized by FT-IR spectroscopy (Fig. 6). The spectrum consists of the typical absorptions of the two interconnected components. Specifically, the P═N vibration mode of the cyclophosphazene core can be seen at 1210 cm^{-1} [24] while the aromatic ring absorptions of the

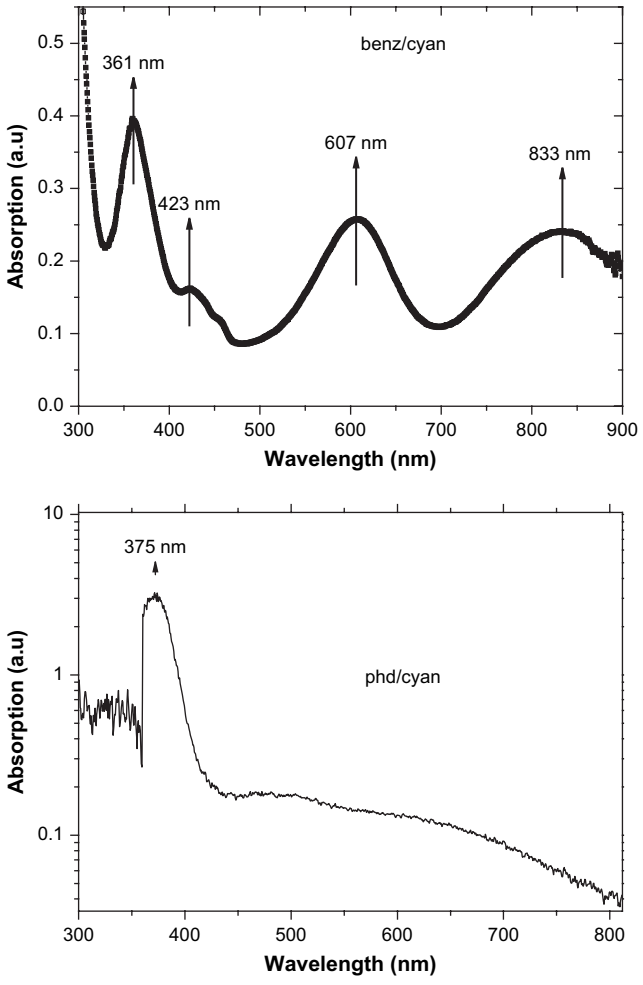

Fig. 5. UV–visible spectra of benz/cyan (aqueous colloidal dispersion, top) and phd/cyan (solid state, bottom).

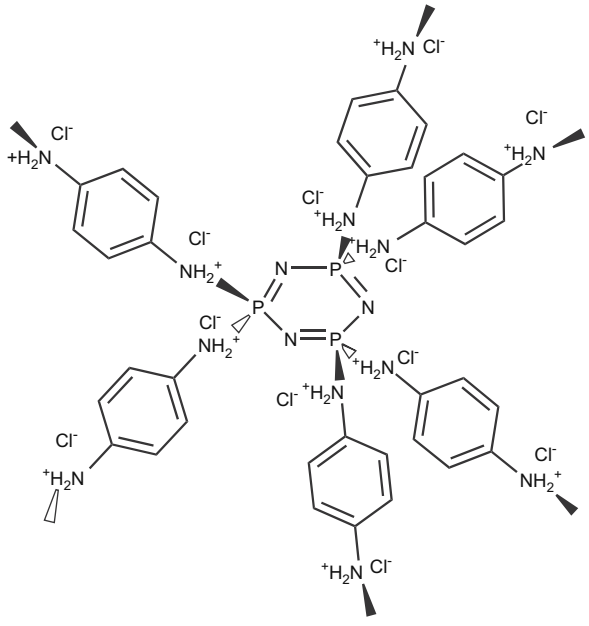

Scheme 1. The proposed structure of the central unit in phd/ptr. The in and out of plane orientations of the diamine ligands is indicated.

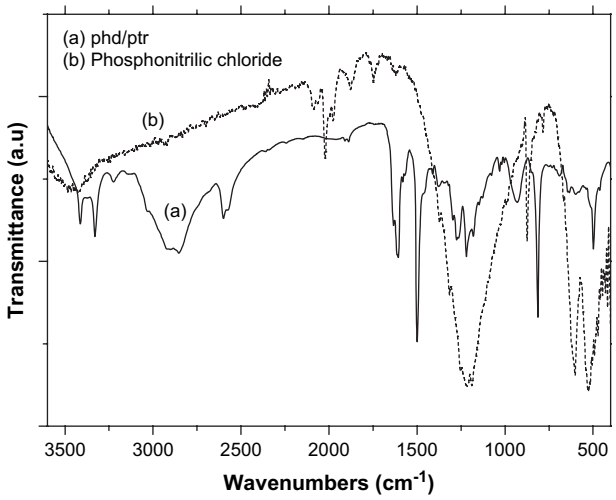

Fig. 6. FT-IR spectrum of phd/ptr in comparison with the phosphonitrilic chloride trimer.

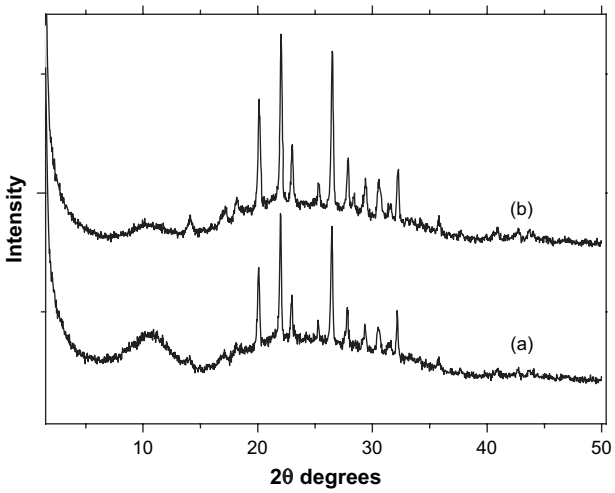

Fig. 8. XRD patterns of (a) phd/ptr and (b) phd/ptr after heat treatment at 175 °C and subsequent cooling at room temperature.

bridging diamine are located at 1600, 1500 and 800 cm^{-1}. The complete nucleophilic substitution of the chlorine atoms in the present case is evidenced mainly by the disappearance of the P–Cl stretching vibration mode at 580 cm^{-1}. Furthermore, the spectrum in the same way with the cyanuric derivatives exhibits the bands of the ammonium cation $-NH_2^+-$ (2600 cm^{-1}) and of the –NH– group (3200 cm^{-1}). The sharp $-NH_2$ vibration modes appear at 3420 and 3320 cm^{-1} while the presence of $-NH_3^+$ groups is marked by a broad absorption band centered at 3000 cm^{-1}.

The thermogravimetric analysis (TGA) diagram of the sample (Fig. 7) shows a two-stage decomposition process. The sample is thermally stable until 180 °C. The first weight loss (40 wt%) between 180 and 275 °C is assigned to the decomposition of the aromatic diamines [2]. The second one is observed above 350 °C, where the thermal degradation of the phosphonitrilic core commences [25].

Since the ligands are expected to be oriented in a 3-D space, the question that arises is if a symmetrical ordering can be achieved or the angle between the diamines leads to an amorphous structure. To this aim, the XRD pattern has been recorded and is presented in Fig. 8. The pattern differentiates from that of the starting crystalline reagents showing various sharp peaks superimposed on a broad amorphous background. On the other hand, the absence of any reflection at $d = 3.5$ Å ($2\theta = 25°$), which is characteristic for π–π stacked phenyl rings [18], pinpoints to a rather open 3-D network. Notably, the reflections appear quite sharp hence indicating the formation of large crystalline domains. In this respect, the structure of the organic network likely resembles that of inorganic zeolites [26].

The modulated DSC diagram (Fig. 9) of phd/ptr shows a melting transition centered at 145 °C (reversible transition), while simultaneously an ordering rearrangement process appears at the non-reversible transition curve. In order to identify if this process forces the network to a more ordered structure, the sample was heated at 175 °C for 30 min, cooled at room temperature and subsequently the XRD pattern was recorded (Fig. 8). The result is indeed an increased ordering, as it is revealed by the significantly reduced intensity of the amorphous broad band centered at $2\theta = 11.5°$ and the increased intensity

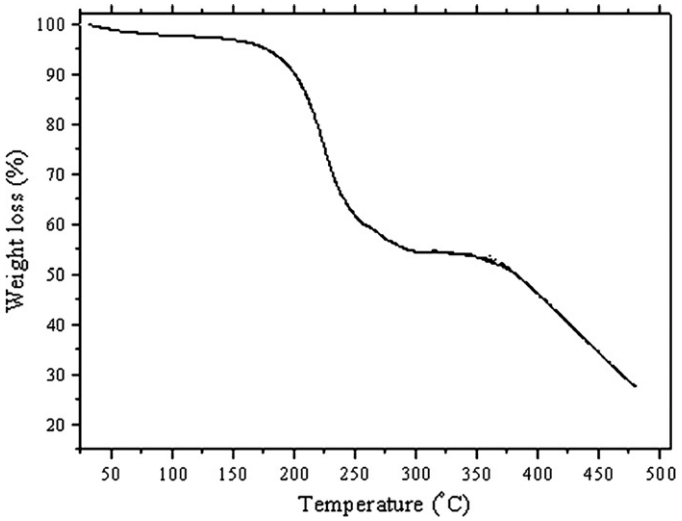

Fig. 7. TGA trace under air of phd/ptr.

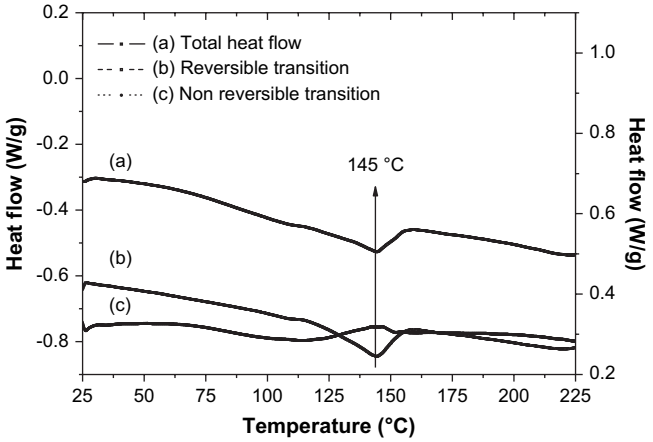

Fig. 9. Modulated DSC diagrams of phd/ptr.

of the sharp crystalline peaks. Similar changes upon heating, including the presence of a melting transition, have been previously reported for other dendritic structures based on phosphonitrilic chloride [27]. The open 3-D structure of the network combined with certain structural defects (e.g. discontinuities) provides enough space for intracrystallite movements of the constituent parts.

The SEM micrographs of phd/ptr (Fig. 10) show mostly cubic shaped particles with sizes ranging from 50 to 200 nm. Nevertheless, a minor fraction of spherical particles can be also observed. The predominant cubic morphology provides strong evidence that these supramolecular assemblies based on the cyclophosphazene cores rather adopt a 3-D symmetry. As mentioned before, the orientation of the chlorine atoms in the phosphonitrilic trimer dictates the particular type of growth. For instance, in the case of the analogous cyanuric chloride derivative one obtains instead a 2-D layered network due to the planar orientation of the replaceable chlorine atoms.

The crystal structure and morphology of an as-designed material is highly depended on the number of phenyl rings in the aromatic diamine in use. When benzidine is used in the place of 1,4-phenylenediamine significant changes in the orientation and symmetry of the network are observed. Accordingly, the benzidine derivative exhibits a markedly less crystalline structure, namely amorphous. In addition, SEM study of this sample revealed an elongated, fibrous morphology. We assign these discrepancies to steric hindrance effects that in turn favour the unidirectional growth of linear chains.

The cyclic voltammetry diagram of phd/ptr is presented in Fig. 11. Similarly, the derivative is electrochemically stable over many cycles exhibiting two reversible redox peaks. Hence, the two oxidation peaks centered at 0.095/0.939 V are accompanied by the corresponding reduction waves centered at −0.493/0.878 V in the reverse scanning direction. In the first step, the initial protonated form is oxidized to the radical cation chloride salt. Subsequently, complete removal of the hydrogen atoms leads to the formation of a quinoid structure similar to that previously proposed for the electrochemically active 1,4-phenylenediamine [20]. The lower first-step oxidation potential of phd/ptr compared with phd/cyan could be ascribed to the carbon substitution in the central triazine core by the more electropositive phosphorus atoms.

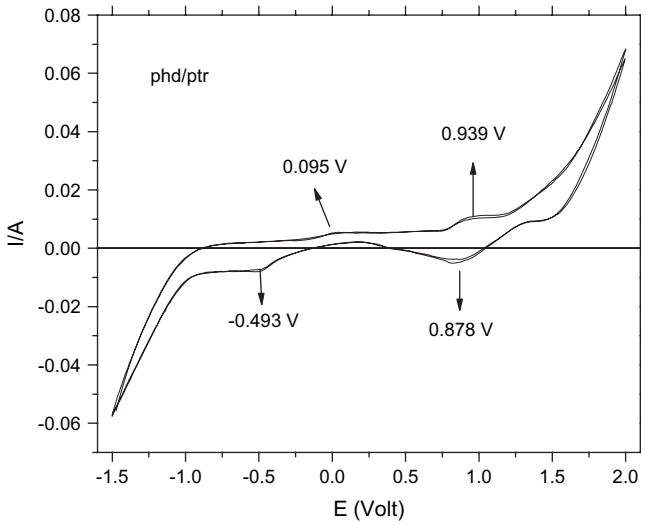

Fig. 11. Cyclic voltammetry diagram of phd/ptr.

The material is virtually insoluble in any solvent, and thus the UV–visible spectrum of phd/ptr was recorded in the solid state (Fig. 12). The spectrum exhibits an intense absorption peak centered at 575 nm that is significantly red-shifted compared to the initial monomers (230–250 nm). This means that some electron delocalization still occurs within the network [6a], albeit the electron overlap cannot be sufficiently high due to the angle between the phosphorus atoms of the triazine core and the nitrogen atoms of the tethered amine ligands. Chemical oxidation of phd/ptr with $(NH_4)_2S_2O_8$ seems to have a deleterious effect in the ordering of the network. Nevertheless, the oxidized solid holds promise as a low band gap optical material. The reaction is rapid while the oxidation proceeds through various steps, each one imparting a different color in the sample. Eventually, the oxidized material reaches a final stable state where the color of the sample is permanently dark red. This sample shows some dispersability in ethanol thus enabling the recording of its optical spectrum (Fig. 12). The spectrum exhibits three distinct absorptions centered at the

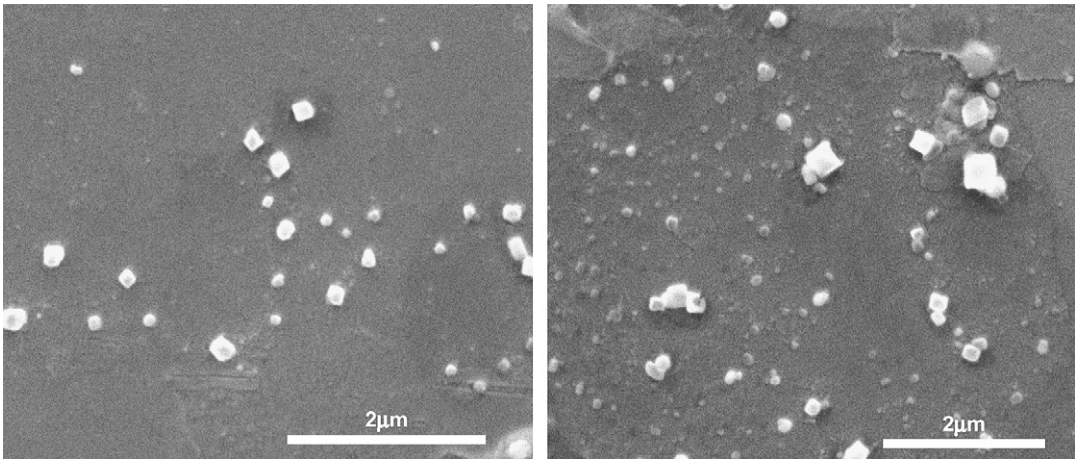

Fig. 10. SEM images of phd/ptr at different sample areas.

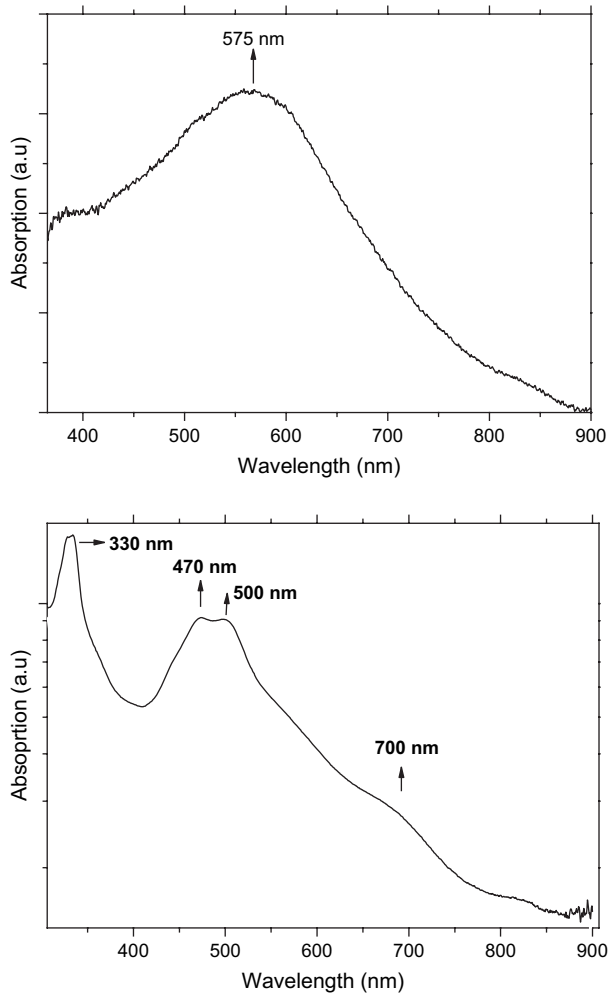

Fig. 12. Top: solid-state UV–visible spectrum of phd/ptr. Bottom: UV–visible spectrum of phd/ptr after oxidation with $(NH_4)_2S_2O_8$. The spectrum has been recorded in ethanol dispersion.

following wavelengths: 500 (energy gap EG = 2.47 eV), 470 (EG = 2.63 eV) and 330 nm (EG = 3.74 eV) as well as a small shoulder at 700 nm of unknown origin. The wavelengths where these absorptions appear and their intensity are relatively low in order to imply the formation of a polaron band. Furthermore the absence of a planar structure does not provide the material with an appreciable orbital overlapping, as in the case of the layered cyanuric chloride derivatives. This is the main reason for the higher energy gaps observed in the case of phosphonitrilic chloride.

4. Conclusions

2-D covalent networks consisting of central cyanuric units or 3-D covalent network consisting of phosphotriazine cores coupled by aromatic diamine bridges have been synthesized and characterized. These molecular building units are versatile tools in the design of novel supramolecular nanostructures with interesting properties. Specifically, the crystalline ordering and the optical properties can be varied according to the type of the diamine ligand or triazine core and the degree of oxidation. Since the ligands are not oriented in a planar conformation in the case of phosphonitrilic molecules, the band gap cannot be sufficiently low and there are no indications for the formation of a polaron band, even if some high wavelength excitations are observed. In contrast, the benzidine/cyanuric chloride couple exhibits significantly low band gap absorptions. On account of their inherited ion-exchange properties, the 2-D and 3-D organic materials resemble conventional inorganic layered and zeolitic solids.

References

[1] Majoral JP, Caminade AM. Chem Rev 1999;99:845–80.
[2] Bourlinos AB, Dallas P, Sanakis Y, Stamopoulos D, Trapalis C, Niarchos D. Eur Polym J 2006;42:2940–8.
[3] Blotny G. Tetrahedron 2006;62:9507–22.
[4] Perdigao LMA, Champness NR, Beton PH. Chem Commun 2006:538–40.
[5] (a) Moriya K, Suzuki T, Kawanishi Y, Masuda T, Mizusaki H, Nakagawa S, et al. Appl Organomet Chem 1998;12:771–9;
(b) Levelut AM, Moriya K. Liq Cryst 1996;20:119–24;
(c) Moriya K, Kawanishi Y, Yano S, Kajiwara M. Chem Commun 2000:1111–2.
[6] (a) Groenendaal L, Bruining MJ, Hendrickx EHJ, Persoons A, Vekemans JAJM, Havinga EE, et al. Chem Mater 1998;10:226–34;
(b) Shahid M, Ashraf RS, Klemm E, Sensfuss S. Macromolecules 2006;39:7844–53;
(c) Christian Pandya HK, Niazimbetova ZI, Beyer FL, Galvin ME. Chem Mater 2007;19:993–1001.
[7] Hancock JM, Gifford AP, Zhu Y, Lou Y, Jenekhe SA. Chem Mater 2006;18:4924–32.
[8] (a) Ajayaghosh A, Eldo J. Org Lett 2001;3:2595–8;
(b) Eldo J, Ajayaghosh A. Chem Mater 2002;14:410–8;
(c) Ajayaghosh A. Acc Chem Res 2005;38:449–59;
(d) Bundgaard E, Krebs FC. Macromolecules 2006;39:2823–31.
[9] Hou J, Tan Z, Yan Y, He Y, Yang C, Li Y. J Am Chem Soc 2006;128:4911–6.
[10] Yang Y, Lowry M, Schowalter CM, Fakayode SOE, Xu X, Zhang H, et al. J Am Chem Soc 2006;128:14081–92.
[11] Shin RYC, Kietzke T, Sudhakar S, Dodabalapur A, Chen ZK, Sellinger A. Chem Mater 2007;19:1892–4.
[12] (a) Brabec CJ, Sarificiftci NS, Hummelen JC. Adv Funct Mater 2001;11:15–26;
(b) Halls JJM, Walsh CA, Greenham NC, Marseglia EA, Friend RH, Moratti SC, et al. Nature 1995;376:498–500;
(c) Kietzke T, Egbe DAM, Hoerhold HH, Neher D. Macromolecules 2006;39:4018–22.
[13] Biswas AK, Ashish A, Tripathi AK, Mohapatra YN, Ajayaghosh A. Macromolecules 2007;40:2657–65.
[14] Kim IT, Elsenbaumer RL. Chem Commun 1998:327–8.
[15] Huang J, Virji S, Weiller BH, Kaner RB. J Am Chem Soc 2003;125:314–5.
[16] Bae WJ, Kim KH, Jo WH, Park YH. Macromolecules 2005;38:1044–7.
[17] Zhang Z, Leinenweber K, Bauer M, Garvie LAJ, McMillan PF, Wolf GH. J Am Chem Soc 2001;123:7788–96.
[18] Lee K, Cho S, Park SH, Heeger AJ, Lee CW, Lee SH. Nature 2006;41:65–8.
[19] Han DH, Park SM. J Phys Chem B 2004;108:13921–7.
[20] Won MS, Shim YB, Park SM. Bull Korean Chem Soc 1992;13:680–3.
[21] Bourlinos AB, Chowdhury SR, Jiang DD, An YU, Zhang Q, Archer LA, et al. Small 2005;1:80–2.
[22] (a) Xia Y, Wiesinger JM, MacDiarmid AG. Chem Mater 1995;7:443–5;
(b) Davey JM, Too CO, Ralph SF, Kane-Maguire LAP, Wallace GG, Partridge AC. Macromolecules 2000;33:7044–50.
[23] (a) Allen CW, Paul IC, Moeller T. J Am Chem Soc 1967;89:6361–2;
(b) Shaw RA, Fitzsimmons BW, Smith BC. Chem Rev 1962;62:247–81.
[24] Barbera J, Bardaji M, Jimenez J, Laguna A, Martinez MP, Oriol L, et al. J Am Chem Soc 2005;127:8994–9002.
[25] Brown DE, Ramachandran K, Carter KR, Allen CW. Macromolecules 2001;34:2870–5.
[26] Bourlinos AB, Zboril R, Petridis D. Microporous Mesoporous Mater 2003;58:155–62.
[27] Barbera J, Jimenez J, Laguna A, Oriol L, Perez S, Serrano JL. Chem Mater 2006;18:5437–45.